TRANSACTIONS ON ELECTROMAGNETIC SPECTRUM

Design and Development of an Electrically Miniature Wideband Monopole Antenna for Wireless Applications

Prasanta Mandal[1*]

[1]Department of Computer Science and Engineering,
Govt. College of Engineering and Textile Technology, Serampore, Hooghly, West Bengal, India
Email: prasanta.anshin@gmail.com

Tapan Mandal[2]

[2]Department of Information Technology,
Govt. College of Engineering and Textile Technology, Serampore, Hooghly, West Bengal, India
Email: tapanmandal20@rediffmail.com

*** Corresponding author's email address:** tapanmandal20@rediffmail.com

Received: 3 April 2023
Revised: 25 April 2023
Accepted: 3 May 2023

Research Article
Vol.2 / No.2 / 2023
Doi: 10.5281/zenodo.7875663

Abstract: An electrically small ($0.32\lambda \times 0.27\lambda \times 0.02\lambda$, where λ is the wavelength at 3.18 GHz), hand fan shaped like microstrip fed planner monopole antenna suitable for use in wireless communication systems is presented. Initially a disk shaped wideband printed antenna is designed. Then the structure is modified to a hand fan like shape. This shape generates higher impedance bandwidth (BW) as compared to the disk shaped. The detailed parametric study is carried out using MoM based IE3D^{TM} simulator. The proposed structure is fabricated for measurement. For proof of concept, experimental results are compared with the simulated one. The measured impedance BW ($|S_{11}|$<-10 dB) of the proposed antenna is 13.44 GHz in the range of 3.18 to 16.62 GHz (135.76 %). The polar radiation patterns are presented at various frequencies within the operating spectrum. Pattern characteristic is omnidirectional in the H-plane and monopole like in the E-plane. The antenna gain lies between 2.54 to 6.16 dB and it has more than 80% efficiency over the whole operating region. This antenna possesses satisfactory results and it is a potential candidate for application in many modern wireless and future 5.8G IoT systems.

Keywords: Monopole antenna, hand fan shape, IoT, UWB, wireless communication.

Cite this paper as: Mandal P., Mandal T., Design and Development of an Electrically Miniature Wideband Monopole Antenna for Wireless Applications. Transactions On Electromagnetic Spectrum. 2023; 2(2): 33-42, Doi: 10.5281/zenodo.7875663

1. INTRODUCTION

In the present scenario, the world is witnessing the era of communications where everyone expects to reach everywhere, whenever he wants and wherever he wants. To reach everywhere in a very short span of time, various types of wireless devices are contemporary requirements in modern lifestyles. To fulfil the requirements, a huge number of wireless-based handy modules are urgent requirement for wireless sensor network operations in the real-time processing services. All the devices are connected in a computer network

that use embedded Internet and Technology. Internet of Things (IoT) enables these devices to be remotely controlled using wireless communication across the network [1]. The Internet connectivity and wireless devices are also required in the areas of (i) smart city, (ii) healthcare industry, (iii) productions, (iv) transportations, (v) remote surveillance, (vi) home automation, and so forth [1-3]. All the wireless communications/wireless sensor network systems require a precise suitable antenna, which is an essential and most important component. Since then lots of research efforts have been initiated and sufficient number of articles have been published in this domain [4-24]. From the literature, it is evident that the printed antenna is a popular candidate for UWB, IoT and many wireless applications due to its admirable benefits (i) wide BW, (ii) low profile, (iii) light weight, (iv) high data rate, (v) stable radiation patterns, (vi) high security, and (vii) flat gain over a wide frequency range, etc. A quantum number of researchers face emerging challenges like wideband impedance matching and good radiation efficiency [5-7, 20].

Apart from the above-mentioned issues, a number of printed ultra-wideband (UWB) antenna designs have been reported in [8-21]. From the articles, it is evident that either microstrip [4 – 11, 22-23] or CPW [11, 15 – 17, 19, 21] feeding line is used to implement this kind of antenna. They are either complex in configurations or large in size with various shapes like rectangular [4-5], square [6], triangular [7], disk [8-10, 18-19], elliptical [9, 24], zero [14], spiral [15], nested polygon [22] and hexagon [16]. Hence, it is quite difficult to incorporate them efficiently within the wireless modules. Small size, simple structure, wide impedance BW along with stable radiation patterns are desirable requirement for modern wireless communication systems.

The integration of several communication standards within a small device is inevitable as space is a constraint. Allocated bands for various communication systems are WiMAX (3.40-3.7 and 5.25-5.85 GHz), WLAN (5.15-5.35 and 5.72-5.85 GHz), ISM (5.725-5.875 GHz), X-band ITU (8.025-8.4 GHz), IoT (5G: 3.4-3.6 GHz and 5.8G Wi-Fi: 5.725-5.825 GHz), UWB (3.1-10.6 GHz), broadcasting satellites (12.4-12.5 GHz), and defense systems (14.62-15.23 GHz) [24-26]. Usually, multiple antennas are used to achieve different standards in wireless systems. The use of multiple antennas will enhance the complexity of the communication systems as well as higher interference over single antenna. Therefore, a simple, small and wideband antenna is a contemporary requirement for use in modern and next generation communication system.

The 5.8G Wi-Fi is more suitable for IoT applications than 2.4G and 5G Wi-Fi due to higher data rate and less interference from the narrow bands [1, 3, 25]. Radio frequency interference grows seriously at 2.4G and 5G Wi-Fi due to consumer demand (almost everywhere around the world today) of wireless devices. In order to connect IoT devices to the internet through 5G and future 5.8G, a simple with electrically miniature monopole antenna is highly desirable due to its high data rate, easy installation and low cost for mass production.

In this paper, a small-size printed UWB antenna has been proposed for use in WiMAX / WLAN / ISM / IoT / UWB / broadcasting satellites / defense, etc. and future 5.8G IoT systems. The design initially begins with a printed disk shape monopole antenna which provides UWB response. The structure is then modified to hand fan like shape to possess wider spectrum. It is small in size, simple in structure and easy to install in various smart wireless devices. To examine the antenna analysis and performance, IE3D^{TM} electromagnetic simulator is used. In order to measured different antenna performances, the proposed design is fabricated. The characteristic of antenna has been studied in terms of frequency and time domain to assess its suitability for wireless communication.

2. ANTENNA GEOMETRY AND DESIGN CONSIDERATION

For this work, a small size ($0.32\lambda \times 0.27\lambda \times 0.02\lambda$) ($30\times25\times1.59$ mm^3) printed antenna is designed on a substrate of thickness, h = 1.59 mm, ε_r = 4.4 and loss tangent, tan δ = 0.02 as depicted in Fig. 1. It shows the stepwise design approaches to evolve from a circular disk (basic shape) to the proposed one. All the elements and design notations of antenna are given in Fig. 1. Each configuration has three sections (i) 50 Ω microstrip fed line for excitation (ii) microstrip patch for radiator and (iii) ground plane for impedance matching. Both the patch and fed line are designed in one side whereas the trapezoidal in shape partial ground plane is printed on the opposite side of the same substrate. A small rectangular in shape slot is truncated at the ground under the fed line for further impedance matching. The lower band edge frequency (f_L) in GHz is computed from the Eqn. (1) [16, 21].

$$f_L = \frac{c}{\lambda} = \frac{7.2}{(L + r + S)} \quad (1)$$

To calculate the f_L of the disk antenna, the height L (in cm) and radius r (in cm) of the effective cylindrical monopole are determined by equating its area as

$$L = 2a \quad (2)$$

$$r = \frac{a}{4} \quad (3)$$

The overall dimensions ($L_s \times W_s$) of the antenna are calculated as

$$L_S = \frac{c}{2f_L\sqrt{\frac{(\varepsilon_r + 1)}{2}}} \quad (4)$$

$$W_S = \frac{\sqrt{3}L_S}{2} \quad (5)$$

where c is the speed of light in vacuum.

By selecting the value of a = 1.0 cm, the design parameters of the disk antenna are found to be as follows: r = 0.25 cm, L = 2 cm, L_s = 2.93 cm and W_s = 2.59 cm. The optimized value of S = 0.085 cm is considered for these calculations. It is possible to fine-tune the calculated values of parameters using the MoM based IE3D simulation software. The calculated and optimized values of f_L are 3.12 and 3.15 GHz respectively. The geometrical parameters after optimization are displayed in Table 1.

Table 1. Design notation of proposed design (in mm)

Notation	L_s	W_s	W_{g1}	W_{g2}	L_g	S	L	W_f	S_1	S_2
Dimension	30	25	19	10.5	7.4	0.85	20	2.8	3	4

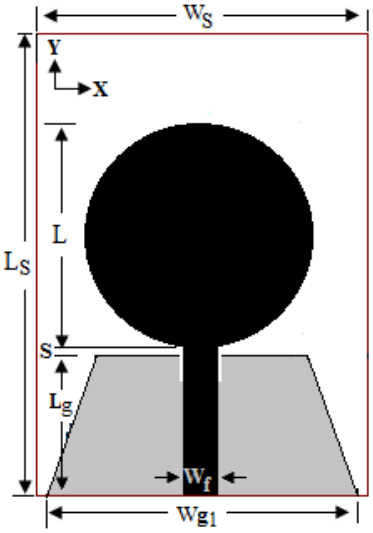

Figure 1. Prototype configuration

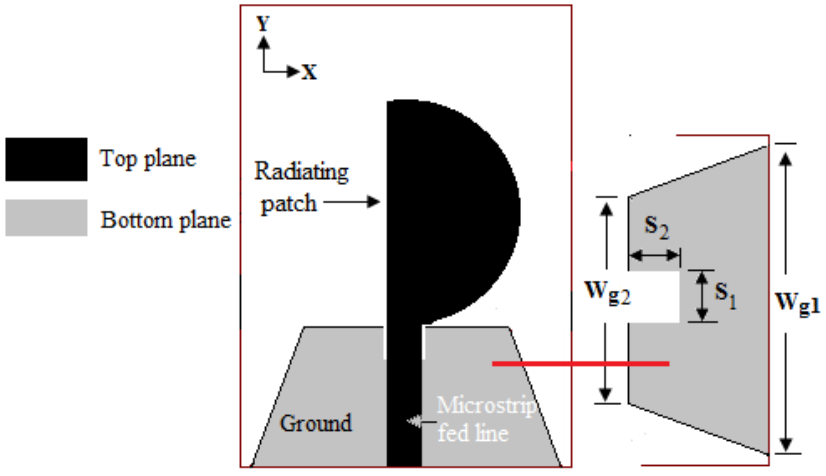

Figure 2. Proposed configuration

The simulated vector current circulation is used to examine the radiation area of an antenna and it gives an idea for antenna design. It helps to determine the electrical dimensions and radiation characteristics accordingly. The length of the half-perimeter of disk is equal to the half wavelength long which is used to determine lower edge frequency of the antenna. Then, almost one-half portion of metal is etched from the disk

patch resulting a hand fan shape radiator, which also provides the same electrical path as the disk. This statement may comply mathematically. From Eq. (1), it is clear that f_L mainly depends on the parameters L, *r*, and *S*. All the parameters are same for both the configurations. Thus, the f_L of the proposed design does not change significantly. The metallic area of the fan shape is smaller than the disk, which is considered as a proposed one (Fig. 2). Therefore, the proposed structure is simple and easy to embed as an internal antenna inside the modern handy wireless integrated devices.

3. PARAMETRIC STUDY AND DISCUSSIONS

The magnitude reflection coefficient ($|S_{11}|$) for different dimensions of disk height (L) and gap (S) between the patch and ground plane are shown respectively in Fig. 3 and Fig. 4. From the Fig. 3, it is observed that as the height increases the lower band edge frequency moves towards the left side of the plot. The reason is that the electrical path length of patch is increasing while height rises. Thus, the lower band edge frequency is shifted and selected by the way of choosing dimension of the disk height. The antenna BW varies remarkably with the variation of the gap (S) between patch and ground as it is evident from the Fig. 4. The gap creates a capacitive load that neutralizes the inductance of the patch resulting in wide BW. Thus, the value of gap is a crucial parameter for the impedance matching. The responses of $|S_{11}|$ versus frequency are portrayed as function of slot width (S_1) and length (S_2) in Fig. 5 and Fig. 6 respectively. From the curves, it is observed that slot parameter has great impact on the impedance matching mainly at the higher frequency region. In order to achieve the best impedance matching at higher frequency, the value of S_1 = 3 mm and S_2 = 3 mm are chosen as the optimum values. The plot of $|S_{11}|$ for a disk and hand fan like shaped configurations is displayed in Fig. 7 for a comparison. It is clear that both the configurations cover the whole UWB range. This modified structure reveals wider impedance BW (13.44 GHz, range: 3.18 - 16.62 GHz) as compared to the prototype design (3.50 - 1.60GHz, range: 3.50 - 1.60GHz) due to good impedance matching. The Fig. 8 provides an illustration for the two parts of input impedance of Fig. 2. From the Fig. 8, it is observed that the real part (resistance) and imaginary part (reactance) fluctuate around 50 Ω and 0 Ω respectively. This behavior of the response states that a good impedance matching has been obtained between the patch and ground plane over a wide spectrum. This hand fan shaped monopole antenna requires less metal than the disk, which may be suitable for use in WiMAX / WLAN / UWB / IoT / etc. wireless systems.

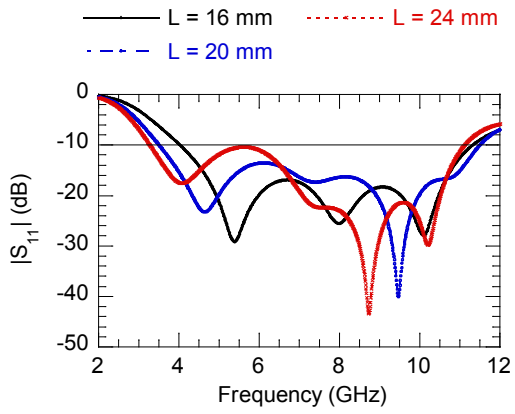

Figure 3. Result of $|S_{11}|$ for different values of disk height (L)

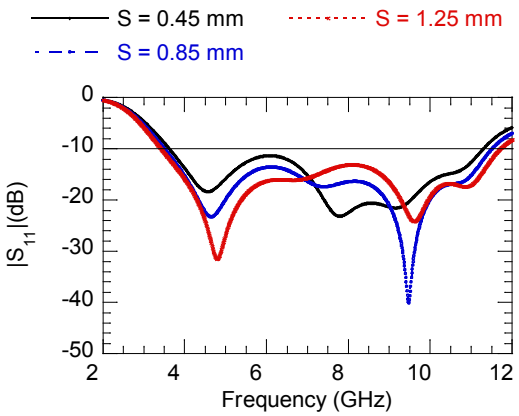

Figure 4. Result of $|S_{11}|$ for different values of gap (S)

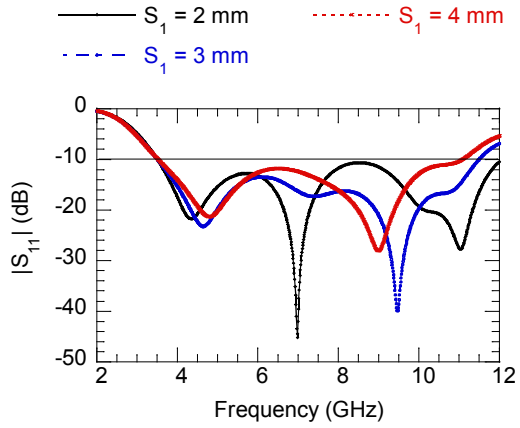

Figure 5. Result of $|S_{11}|$ for different values of slot width (S_1)

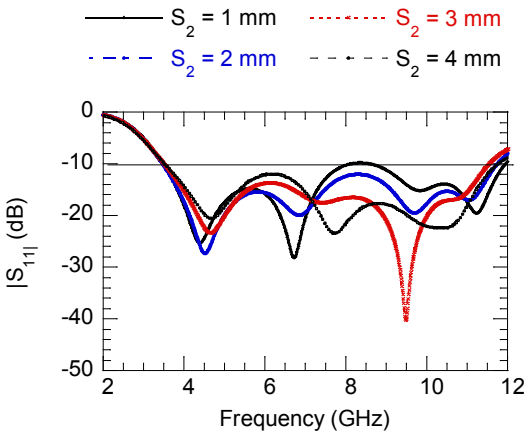

Figure 6. Result of $|S_{11}|$ for different values of slot length (S_2)

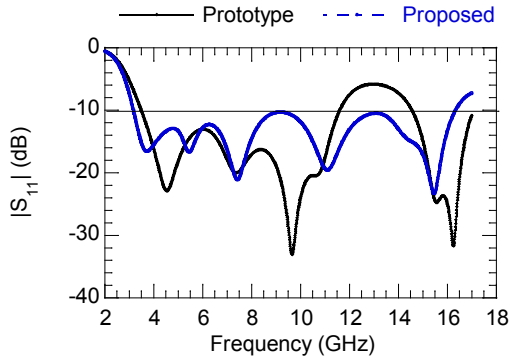

Figure 7. Result of $|S_{11}|$ of different structures for comparison

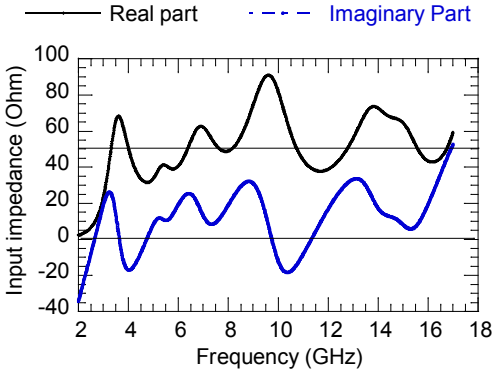

Figure 8. Result of input impedance of proposed antenna

4. MEASURED RESULTS

4.1. Frequency Domain

For the proof of concept, the antenna is fabricated with parameters tabulated in Table 1 and is shown in Fig. 9. The antenna performance is tested using Agilent make (Model: N5230A) vector network analyzer. Fig. 10 and 11 show the comparative graphs of S-parameters. From the Fig. 11, the simulated and measured BW of the proposed antenna exhibit a wideband performance from 3.15 to 16.38 GHz (135.31%) and from 3.18 to 16.62 GHz (135.76 %) respectively for $|S_{11}| \leq$ -10dB. A good alliance is observed between the responses. The numerical and experimental responses of the proposed antenna gain and efficiency are shown respectively in Fig. 12 and Fig. 13. It reveals that the antenna gain has nominal variation and antenna efficiency is more than 80% over wide spectrum range. However, the prototype antenna has higher gain and efficiency due to more metallic area over the proposed one. The radiation patterns at different frequencies are shown in Fig. 14 for a comparison. From the Fig. 14, it is evident that the simulated results for both configurations are almost identical and the numerical performances of the proposed configuration comply with the measured one. The E-plane and H-plane patterns are figure of eight and zero in shape respectively. Both the patterns deteriorate at higher frequencies due to higher mode excitation by the structure. The minor differences between the simulated and experimental results are mostly due to (i) fabrication tolerances (ii) wide flange of SMA connector and (iii) solder iron. However, the good omni-directional H-plane patterns are stable throughout the whole operating region. Thus this small size, hand fan shape configuration may be a potential candidate for the modern wireless applications.

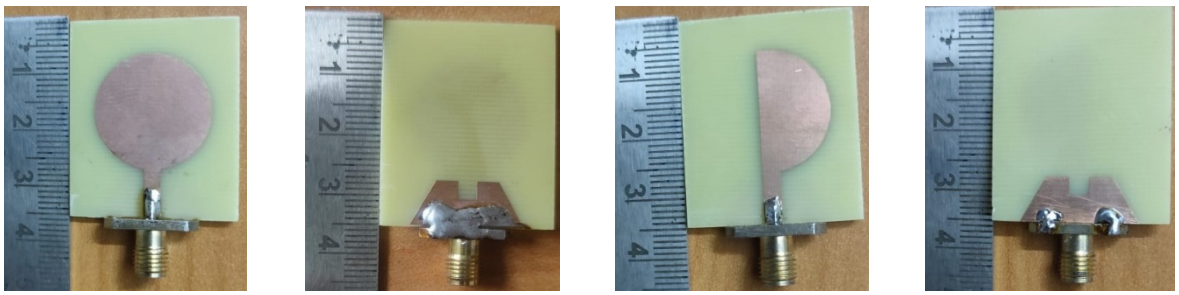

(a) top (b) bottom (c) top (d) bottom

Figure 9. Photograph of fabricated (a) prototype (b) proposed antenna

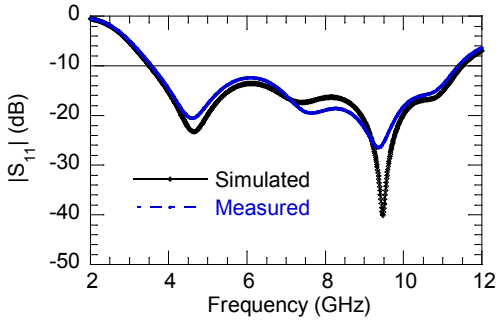

Figure 10. Result of S-parameter of Fig. 9(a)

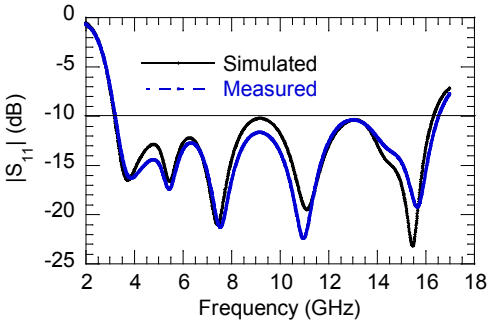

Figure 11. Plot of S-parameter of 9(b)

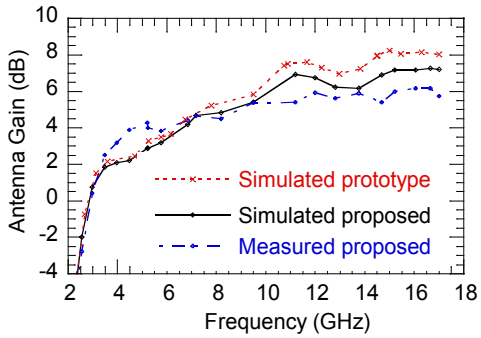

Figure 12. Result of antenna gain

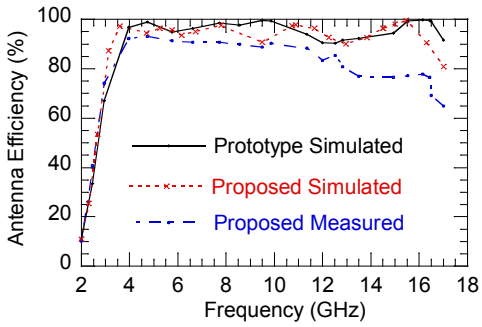

Figure 13. Result of antenna efficiency

(a) 3.54 GHz

(b) 5.5 GHz

(c) 9.5 GHz

(d) 14.4 GHz

Figure 14. Radiation patterns of prototype and proposed antenna, —×— simulated (prototype); - -o- - simulated (proposed); ····●···· measured (proposed)

4.2. Time Domain

Transfer function and group delay for face to face mode is demonstrated in Fig. 15. The variation of S_{21} is little (less than 15 dB) from 3.18 to 16.62 GHz while the variation of group delay (Fig. 15) for Fig. 9(b) is within 4 ns across the whole operating band. The group delay has well parity to the magnitude of S_{21}. It confirms that the antenna has a satisfactory time domain response and a small pulse distortion between transmitted and received signal. Measured phase versus frequency response of the proposed antenna is shown in Fig. 16. From the response, it is found that the phase is linear across the operating frequency region. Thus, it is suitable for application in various modern wireless communications.

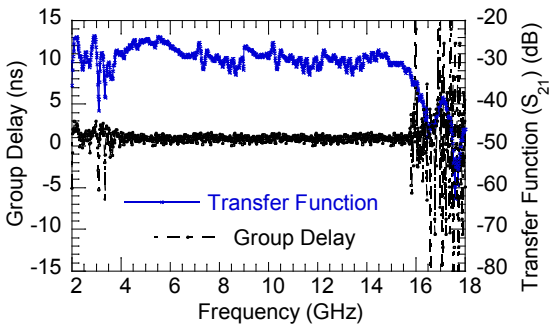

Figure 15. Measured Group delay and S_{21}(dB) of Fig. 9(b)

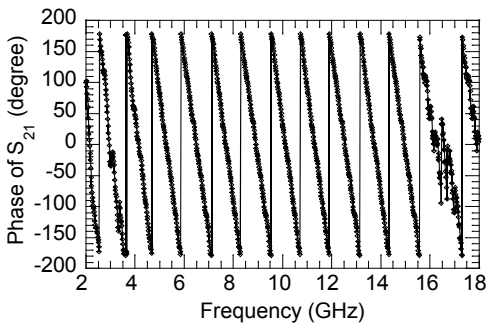

Figure 16. Measured phase of Fig. 9(b)

5. CURRENT DISTRIBUTION ANALYSIS

In the cavity model, the cavity is the interior section between the patch and ground. The electric and magnetic walls are bounded respectively on the top – ground layer and all along the periphery. The magnetic field distribution exists only in the vertical direction of the proposed geometry. There is no tangential magnetic field in the perfect magnetic wall (PMW) but the magnetic field is present normal to PMW. The simulated current distribution of both antennas at different frequencies is shown in Fig. 17. It can be seen that the currents are mainly distributed along the periphery of the patch whereas a little amount of currents appears in the central region. The prototype antenna has symmetrical current distributions with respect to the feed line due to even mode excitation. Thus, the vertical symmetrical line (Y-Z plane) acts as open circuit (magnetic wall). Then almost the one-half portion of metal is removed from the prototype structure along the vertical line, which does not affect the current flow along the curved perimeter of the modified structure. This leads to almost 50% reduction of metallic area. This modified structure provides higher impedance BW due to the generation of another resonant frequency at higher frequency range. This resonant frequency is created due to the current distribution of vertical path from the feed to end point of patch. At lower frequency region of operating band, the currents are uniformly distributed within the patch and flow of current is along the vertical direction which makes the antenna a good radiator. As frequency increases, the H-plane patterns are nearly the same as the lower frequency patterns but E – plane patterns show more changes due to (i) arbitrary current distributions in the radiating patch for the higher mode excitation by the structure (ii) Jx component of current in the ground and (iii) small size of ground plane.

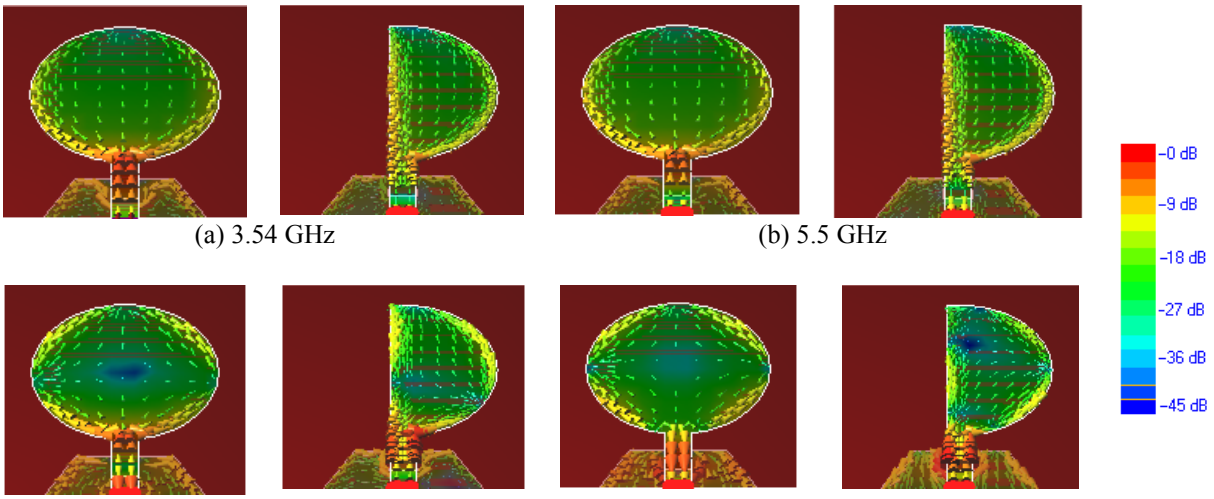

(a) 3.54 GHz (b) 5.5 GHz

(c) 9.5 GHz (d) 10.5 GHz

Figure 17. Simulated current distribution for comparisons

6. BDR CALCULATION

Bandwidth Dimension Ratio (BDR) [27] is expressed by the BW and antenna size. It is calculated using the formula.

$$\text{BDR} = \frac{\text{antenna BW(\%)}}{\text{electrical length} \times \text{electrical width}} \tag{6}$$

The lower band edge wavelength (λ) is used to determine the electrical length and width. The proposed antenna has the measured impedance BW of 135.76% along with high BDR of 1610.98. A comparative study has been made in Table 2. From Table 2, it is revealed that the proposed design has better performance in comparison with the earlier published articles.

Table 2. Comparison of proposed design with published article

Ref	ε_r /h	f_L in GHz	BW (%)	BW ratio	Electrical dimension in λ^2	BDR
[5]	3.48/0.76	3.10	112.06	3.55:1	0.33×0.27	1264.34
[6]	3.50/1.00	2.61	61.09	1.88:1	0.45×0.09	1571.33
[7]	4.70/1.00	2.99	109.87	3.44:1	0.40×0.30	921.73
[8]	4.40/1.60	2.10	146.15	6.43:1	0.38×0.25	1578.16
[9]	2.65/1.00	2.90	122.15	4.14:1	0.40×0.33	940.00
[10]	2.65/1.50	2.96	120.86	4.05:1	0.37×0.24	1361.24
[11]	4.70/1.50	3.46	103.62	3.15:1	0.58×0.50	362.33
[12]	4.40/1.00	3.10	109.49	3.42:1	0.47×0.33	712.08
[13]	4.32/1.52	3.90	112.85	3.59:1	0.46×0.39	635.95
[15]	3.55/0.51	3.74	94.65	2.80:1	0.62×0.50	304.50
[16]	4.40/1.59	2.87	131.26	4.82:1	0.40×0.34	948.53
[17]	4.40/1.59	3.03	121.15	4.07:1	0.42×0.32	894.26
[18]	4.40/1.50	3.30	105.04	3.21:1	0.44×0.42	571.10
[19]	2.33/1.58	2.60	122.39	4.15:1	0.43×0.43	651.77
This work	4.40/1.59	3.18	135.76	5.23:1	0.32×0.27	1610.98

7. CONCLUSION

A miniature microstrip fed simple printed antenna has been designed, investigated, and proposed. The simulated current distributions and design equations are used to ensure the simultaneously a reduction metallic area of the proposed design and analysis. Proposed antenna is successfully fabricated and tested. The characteristics of the tested responses have good agreement with the simulated one. The simulated and measured results of proposed antenna operate in the range of 3.15 to 16.38 GHz (135.31%) and 3.18 to 16.62 GHz (135.76%) respectively. The proposed antenna exhibits omni-directional radiation characteristics, appreciable antenna gain and efficiency and has linear phase of transfer function and almost constant group delay within the operating range. Thus, the proposed antenna is a suitable candidate for applications in WiMAX / WLAN / ISM / IoT / UWB / broadcasting satellites / defense systems, etc. as it meets desire requirements.

REFERENCES

[1] De A, Roy B, Bhattacharjee AK. Miniaturized dual band consumer transceiver antenna for 5G-enabled IoT-based home applications. International Journal of Communication Systems. 2021;34(11):e4840.

[2] Bekasiewicz A, Koziel S. Compact UWB monopole antenna for internet of things applications. Electronics Letters. 2016;52(7):492-4.

[3] Mao Y, Guo S, Chen M. Compact dual-band monopole antenna with defected ground plane for Internet of things. IET Microwaves, Antennas & Propagation. 2018;12(8):1332-8.

[4] John M, Ammann M. Optimization of impedance bandwidth for the printed rectangular monopole antenna. microwave and optical technology letters. 2005;47(2):153-4.

[5] Chung K, Kim J, Choi J. Wideband microstrip-fed monopole antenna having frequency band-notch function. IEEE Microwave and Wireless Components Letters. 2005;15(11):766-8.

[6] Meng L, Wang W, Su M, Gao J, Liu Y. Bandwidth extension of a printed square monopole antenna loaded with periodic parallel-plate lines. International Journal of Antennas and Propagation. 2017;2017.

[7] Lin C-C, Chuang H-R. A 3-12 GHz UWB planar triangular monopole antenna with ridged ground-plane. Progress In Electromagnetics Research. 2008;83:307-21.

[8] Kumar R, Sinha R, Choubey A, Mahto SK. An ultrawide band monopole antenna using hexagonal-square shaped fractal geometry. Journal of Electromagnetic Waves and Applications. 2021;35(2):233-44.

[9] Liu J, Gong S, Xu Y, Zhang X, Feng C, Qi N. Compact printed ultra-wideband monopole antenna with dual band-notched characteristics. Electronics letters. 2008;44(12):710-1.

[10] Yang C, Guo Q, Huang K. Study of a Double–Fed Circular Disc Monopole Antenna for UWB Systems. Journal of Electromagnetic Waves and Applications. 2010;24(14-15):1943-52.

[11] Li P, Liang J, Chen X. Study of printed elliptical/circular slot antennas for ultrawideband applications. IEEE Transactions on antennas and Propagation. 2006;54(6):1670-5.

[12] Zhan K, Guo Q, Huang K. A miniature planar antenna for Bluetooth and UWB applications. Journal of Electromagnetic Waves and Applications. 2010;24(16):2299-308.

[13] Hayouni M, Choubani F, Vuong T-H, David J. Main effects ensured by symmetric circular slots etched on the radiating patch of a compact monopole antenna on the impedance bandwidth and radiation patterns. Wireless Personal Communications. 2017;95:4243-56.

[14] Srivastava K, Kumar A, Kanaujia BK, Dwari S, Kumar S. Multiband integrated wideband antenna for bluetooth/WLAN applications. AEU-International Journal of Electronics and Communications. 2018;89:77-84.

[15] Omar A, Shubair R, editors. UWB coplanar waveguide-fed-coplanar strips spiral antenna. 2016 10th European Conference on Antennas and Propagation (EuCAP); 2016: IEEE.

[16] Mandal T, Das S. Design of a CPW fed simple hexagonal shape UWB antenna with WLAN and WiMAX band rejection characteristics. Journal of Computational Electronics. 2015;14:300-8.

[17] Chakraborty M, Pal S, Chattoraj N. Quad notch UWB antenna using combination of slots and split-ring resonator. International Journal of RF and Microwave Computer-Aided Engineering. 2020;30(3):e22086.

[18] Bhavarthe PP, Rathod SS, Reddy K. A compact dual band gap electromagnetic band gap structure. IEEE Transactions on Antennas and Propagation. 2018;67(1):596-600.

[19] Siddiqui JY, Saha C, Antar YM. Compact SRR loaded UWB circular monopole antenna with frequency notch characteristics. IEEE Transactions on Antennas and Propagation. 2014;62(8):4015-20.

[20] Kimouche H, Abed D, Atrouz B, Aksas R. Bandwidth enhancement of rectangular monopole antenna using modified semi-elliptical ground plane and slots. Microwave and Optical Technology Letters. 2010;52(1):54-8.

[21] Ray K, Tiwari S. Ultra wideband printed hexagonal monopole antennas. IET microwaves, antennas & propagation. 2010;4(4):437-45.

[22] Ak HH. On-Body Monopole Antenna Design and Analyses for the UWB Applications. Transactions On Electromagnetic Spectrum. 2022;1(1):19-23.

[23] Hedayati P. Ultra Wideband Elliptic Monopole Antenna. Transactions On Electromagnetic Spectrum. 2022;1(1):14-8.

[24] Ejaz W, Anpalagan A, Imran MA, Jo M, Naeem M, Qaisar SB, et al. Internet of Things (IoT) in 5G wireless communications. IEEE Access. 2016;4:10310-4.

[25] Pan J, Zhang L, Liu C, Liu H, Okuno Y, editors. A novel compact Printed Inverted-F MIMO antenna operating at 5.8 GHz for WiFi applications. 2016 Progress in Electromagnetic Research Symposium (PIERS); 2016: IEEE.

[26] Kulkarni J, Kulkarni N, Desai A. Development of "H-Shaped" monopole antenna for IEEE 802.11 a and HIPERLAN 2 applications in the laptop computer. International Journal of RF and Microwave Computer-Aided Engineering. 2020;30(7):e22233.

[27] Tiwari RN, Singh P, Kanaujia BK. A half cut design of low profile UWB planar antenna for DCS/PCS/WLAN applications. International Journal of RF and Microwave Computer-Aided Engineering. 2019;29(9):e21817.

